

Structure Transition in PSS/Lysozyme Complexes: A Chain-Conformation-Driven Process, as Directly Seen by Small Angle Neutron Scattering

J  r  mie Gummel, Fabrice Cousin,* and Fran  ois Bou  

Laboratoire L  on Brillouin, CEA Saclay 91191 Gif-sur-Yvette Cedex, France

Received October 8, 2007; Revised Manuscript Received December 21, 2007

ABSTRACT: Measurements of chain conformation in protein/polyelectrolyte complexes (lysozyme and PSSNa) show that the crossover observed between an open structure, a chain network cross-linked by the proteins, and a globular one, dense globules of ~ 10 nm aggregated in a fractal way, results from a conformation modification prior to the transition. Before showing this, we have widened the parameter range for the observation of the transition. We had shown before that the two structures can be formed depending on chain length (for a given [PSS]/[lysozyme] ratio): gel for large chains, globules for short chains. We show here that the crossover between these two regimes can also be reached as a function of the chain concentration or the salinity of the buffer. Since all of these crossover parameters act on chains overlapping concentration c^* , we reinforce the idea of a transition from the dilute to the semidilute regime, but c^* is shifted compared to pure PSS solutions. In order to understand this, we have measured by SANS the conformation of a single chain of PSS in the presence of proteins within the complexes. This is achieved by a specific labeling trick where we take advantage of the fact that lysozyme and hydrogenated PSS chains have the same neutron scattering length density. In the gel structure, the PSS chains keep a wormlike structure as in pure solutions, but their persistence length is strongly reduced, from 50   without proteins to 20   on average with lysozyme. With this value of 20  , we calculate new overlapping thresholds (concentration, mass, ionic strength) in agreement with observed ones. In a second stage, after the globular structure is formed, the PSS chains get a third conformation, no longer wormlike but more collapsed, within the globules.

I. Introduction

The science of complexes of polyelectrolytes with proteins in aqueous solvents is presently widening and progressing, prompted by its importance in real life (food, biotechnology and biology, personal care, and physicochemical control of various processes). We focus here on electrostatic complexes, resulting from association between two species of opposite electric charges. Understanding the structure of these complexes is quite relevant. Beyond imaginative pictures extrapolated from information at the macroscopic scale,^{1–3} progress has been done via techniques at scales characteristic of the structure. We have shown recently in a series of papers^{4–6} that neutron scattering, complemented by imaging for larger scale, using FFTEM (freeze fracture),⁷ provides much crucial information. The very “technique-convenient” system we used is a mixture of lysozyme, a model globular protein (positive global charge), with sodium poly(styrene sulfonate), PSSNa (negatively charged). This is convenient because the chains can be labeled by deuteration. The key point of these recent studies was that, owing to deuterium labeling for neutron radiation, we could measure separately the scattering from protein and from polymer and therefore their spatial arrangement.

We actually observed three different structures, corresponding to three regions of the state diagram established from visual and rheological observation. Among the three, two are probably common to many systems, as inferred from macroscopic or light scattering experiment measurements^{1,2} (the third structure, optically clear, shows lysozyme unfolding by a large PSS-to-lysozyme ratio, a phenomenon encountered at room temperature with PSSNa only). Among the two general structures, the **first structure** shows chains spreading all over the solvent (like in solution) but connected by the proteins which act as individual cross-links. This structure presents a soft elasticity; hence, we

call it a gel. Such a gel-like structure has been observed within BSA/PDMAC coacervates⁸ or with hydrophobically modified poly(sodium acrylate) reversibly cross-linked with proteins.⁹ The **second structure** is liquid, but at a small scale, it is much more heterogeneous than the first one. It is made of primary globules with a narrow size distribution (peak value of 10–30 nm depending on the electrostatic parameters), which contain both proteins and chains, at a rather high compactness. These globules aggregate at a higher scale in ramified bunches, with a fractal dimension of 2.1 like the result of a reaction limited aggregation process. Eventually, very large aggregates precipitate at long times. The local organization in globules is common to many systems involving polyelectrolytes and spheres of opposite charges, including complexes made of proteins and polyelectrolytes^{1,2,10–12} (the higher scale organization, fractal in our case, seems more system dependent, as coacervates are often observed in close systems) as well as other systems such as complexes made of polyelectrolyte-neutral diblock copolymers and micelles,^{13,14} complexes made of polyelectrolytes and micelles,¹⁵ or complexes of polyelectrolytes and inorganic charged nanoparticles.¹⁶

Obviously, gel and globule structures are also very different from many macroscopic points of view (rheology, transport, electrophoretic behavior, permeability, species access, response to dilution, stability). Thus, it is important in practice to control the transition from one to another. The similarity between the structure of the PSS chains within the gel structure and within pure solutions of PSS chains in the semidilute regime prompted us to imagine in ref 4 that the physical origin of the crossover between the two regimes is the state of interpenetration of the chains after interaction with the proteins: if chains are interpenetrated (semidilute regime), they could easily be cross-linked by the proteins and form a gel, which in turn prevents them from collapsing into globules.

We also showed in our first measurements⁴ that the gel–globule crossover limit as a function of chain length **does**

* Corresponding author. E-mail: Fabrice.Cousin@cea.fr.

not correspond to the chain overlapping limit, c^* , if we calculate it assuming the same chain conformation as that in polyelectrolyte solutions, which has been determined, for example, in ref 17. This was in accordance with the fact that the PSS chains were shrunk in the presence of the proteins.

This leads us to the explanation that the **chain conformation is modified under addition of proteins**; this would in turn change c^* . It has been, for example, shown recently by light scattering and viscosity measurements¹⁸ that, for PAA, under addition of oppositely charged micelles (similar in shape to globular proteins), c^* is shifted toward higher concentrations by a factor 5. Such an influence of the addition of oppositely charged pearl-like objects on the overlapping concentration of charged stringlike objects has not yet been described, to our knowledge, by theories or simulations. Although there is now a lot of literature dealing with the adsorption of a polyelectrolyte on an oppositely charged sphere as a function of the chain stiffness, chain length, ionic concentration, particle size, and surface charge density (see, for example, the review of Ulrich et al.¹⁹), the simulations cannot yet involve enough objects to resolve overlapping chain concentration problems.

Simulations^{20,21} show that the binding of spherical macroions on polyelectrolytes decreases when the stiffness of the chain increases. Experimentally, this has been confirmed in ref 22 by turbidity measurements on micelle/polyelectrolyte and protein/polyelectrolyte systems. We believe thus that the c^* value of polyelectrolytes would be less affected by complexation for stiff chains. We recall here that PSS has a very small bare persistence length ($\sim 10 \text{ \AA}$ ^{17,23,24}). Its c^* should thus be strongly influenced by complexation. It has to be noted that a strong increase of salt may lead to release of macroions from the chains due to the screening of electrostatic interactions.²¹ In this case, the c^* value of the chains should correspond to the one of the pure polyelectrolyte solutions. Nevertheless, simulations involving several chains or several spheres begin to appear. They lead to dense or open aggregates, resembling the globular or gel-like observed structures^{25,26}. In these simulations, these differences in structure depend on the strength of interactions and not on the dilution state of the chains.

In order to check that the concentration crossover is directly linked to c^* , we propose to measure in the present paper directly the conformation of chains in the presence of proteins inside the complexes. It happens that this is possible, in our system, using neutron scattering. This is due to some fortunate scattering specificity of the components of our system: non-deuterated PSS and lysozyme have the same neutronic contrast, so they can both be matched by the same $\text{H}_2\text{O}/\text{D}_2\text{O}$ mixture. Meanwhile, deuterated PSS is not matched and still visible in this mixture. This particularity will enable us to determine the form factor of the individual chain.

For the sake of consistency between our former work and the present one, the content of the paper is twofolded: (1) One fold reports results using the former method: By contrast matching of either polymer or protein, we probe the gel–globule transition over a larger range of chain concentrations and ionic strengths. This part being not principal here, some of the data will be presented in the Appendix. (2) The second fold reports on an original method: The direct measurement of the conformation of the PSS chains in both the gel structure and the globular structure. Results show how the evolution of chain conformation, first from solution to gel and second to globule, is indeed here the key for the transition.

II. Material and Methods

1. Sample Preparation. The synthesis of poly(styrene sulfonate) is done in several steps. We first purchase from Polymers Standards Service poly(styrene) chains of 800 repeating units ($M_w = 90000$),

with very low polydispersity ($M_w/M_n = 1.03$), in non-deuterated and deuterated versions (for contrast matching SANS studies). A post-sulfonation of these chains grafts the sulfonate groups on the aromatic cycles. This is a derivation of Makowski's method.²⁷ A reactive species, created in situ by the reaction between sulfuric acid and acetic anhydride, attacks the aromatic cycle, which grafts the sulfonate group in the para position (not the ortho position due to the chain backbone steric hindrance). The poly(styrenic acid) solution is then neutralized by NaOH to obtain a PSSNa solution. This solution is then dialyzed against deionized water. The dialysis is monitored by conductivity, and water is renewed as many times as necessary until reaching the conductivity of pure water ($18 \text{ M}\Omega$). The solution is concentrated in a rotating evaporator and finally freeze-dried, yielding a white powder that can be stored. The sulfonation rate of PSS chains, f , can be accurately measured by SANS (not shown here). It is well-known that the value of the correlation peak q^* of pure solutions of PSSNa depends on f in a reproducible way when all chains are labeled with respect to solvent. For 0.3 mol/L , one gets $q^* = 0.1 \text{ \AA}^{-1}$ ^{17,28,29}

Lysozyme is purchased from Sigma, and the same lot has been used for all of our studies, without further purification. All samples are made in an acetic acid/sodium acetate buffer solution to reach a pH of 4.7. The buffer concentration is always first set to have an ionic strength of $5 \times 10^{-2} \text{ mol/L}$. For specific experiments, the ionic strength of the buffer is increased to 1×10^{-1} , 2×10^{-1} , or $5 \times 10^{-1} \text{ mol/L}$ by addition of NaCl.

Two solutions, one of lysozyme and one of PSS, are first prepared separately in the acetic buffer at twice the concentrations wanted. For the measurements of the PSS chain conformation, the PSS solution contains hydrogenated and deuterated PSS chains, mixed together in the ratio PSS_H/PSS_D wanted, before mixing with the protein. The two solutions, PSS and protein, are then quickly mixed and slightly shaken to be homogenized. The samples are then left for 2 days at rest; we checked in previous experiments that this is enough to reach a stable state. We define a charge ratio introduced noted $[-]/[+]_{\text{intro}}$ which is obtained as a function of the concentrations introduced, taking for the net charge of the lysozyme a value of +11 (at pH 4.7) and for the charge of the PSS one negative charge per monomer. This ratio thus corresponds to the structural charges and not to the effective charges predicted for free chains by Manning's condensation. The charge ratio $[-]/[+]_{\text{intro}}$ used here is generally 3.33 (40 g/L of protein and 0.1 mol/L of PSS repeating units). $[-]/[+]_{\text{intro}}$ is varied only in experiments for which the concentration of PSS chains is changed at constant concentration of protein (40 g/L, Figure 8 in the Appendix).

2. SANS Experiments. SANS measurements were done on the SANS spectrometers PAXY and PACE (LLB, Saclay, France) in a q range lying from 6×10^{-3} to $3 \times 10^{-1} \text{ \AA}^{-1}$. All measurements were done under atmospheric pressure and at room temperature. For SANS experiments concerning the determination of the threshold of the transition between the gel and the aggregates of globular complex regimes, hydrogenated protein and deuterated PSS have been used, like in our previous experiments^{4,5}. Each sample was achieved either in a 57%/43% $\text{H}_2\text{O}/\text{D}_2\text{O}$ mixture that matches the neutron scattering length density of lysozyme to get the PSS signal or in a 100% D_2O solvent that matches the neutron scattering length density of PSS to get the signal of the lysozyme. For the measurements of the conformation of the PSS chains, hydrogenated protein and a mixture of hydrogenated and deuterated PSS have been used. In order to get only the signal of deuterated PSS chains, each sample was made in a 57%/43% $\text{H}_2\text{O}/\text{D}_2\text{O}$ mixture that matches both the neutron scattering length density of lysozyme and hydrogenated PSS. Table 1 recalls all of the scattering density lengths of the species and solvents used in the different experiments.

Standard corrections for sample volume, neutron beam transmission, empty cell signal subtraction, detector efficiency, subtraction of incoherent scattering, and solvent buffer scattering were applied to get the scattered intensities in "absolute units" (cm^{-1}).

Table 1. Scattering Length Densities of the Different Species and Solvent Used in the Experiment

	lysozyme ^a	h-PSS chains	d-PSS chains	57%/43% H ₂ O/D ₂ O	100% D ₂ O
ρ (cm ⁻²)	2.52×10^{10}	2.52×10^{10}	6.26×10^{10}	2.52×10^{10}	6.39×10^{10}

^a This value corresponds to the value in a 57%/43% H₂O/D₂O mixture and takes into account the exchange of the labile hydrogen at the surface of the protein with the solvent.

III. SANS from Protein or Polymer: More Parameters for the Gel-to-Globule Transition

Before showing the form factor measurements in section IV, we report in this section new data for SANS from protein (polymer matched) or polymer (protein matched) generalizing our former study^{4,5}. As before, we consider cases where the charges brought by each component $[-]/[+]_{\text{intro}}$ are of the order of 1 (between 0.5 and 3.33).

1. Results. 1.a. Effect of Chain Length. We first recall here former results on the influence of the chain length^{4,5}. In this work, we had kept all other parameters constant, namely, a concentration of 0.1 M for the PSS chains and 40 g/L for lysozyme ($[-]/[+]_{\text{intro}} = 3.33$) and an ionic strength of 5×10^{-2} M. These former results⁴ are presented in Figure 1, together with new results detailed just below. The signals of proteins (matching PSS) and of PSS chains (matching proteins) are plotted separately. Differences between short and long are clear-cut:

For small chains of $N = 50$,⁵ $N = 90$, and $N = 360$,⁴ spectra are characteristic of aggregates of globular structures. Lysozyme scattering and PSS scattering have the same features because both species objects are embedded in the globules. We get a strong correlation peak at 0.2 \AA^{-1} corresponding to contact distance between two proteins, a second q^{-4} behavior at

intermediate q corresponding to the form factor of the primary compact complexes and a $q^{-2.1}$ behavior at low q corresponding to the larger scale fractal organization of the primary complexes (please note that an exponent of 2.5 was first reported in ref 4 but later measurements at low q^5 enabled us to refine the value to 2.1).

For longer chains ($N = 625^4$), the behavior is drastically different. The lysozyme and PSS scatterings are no longer similar. The protein spectra show that proteins are distributed randomly at a small scale and heterogeneously at a higher scale with a fractal dimension ($D_f = 2.5$) akin to spatial distribution of cross-linkers observed in some cases in gels.³⁰ The PSS chain spectra show that the transient network formed by PSS chains alone in solution remains because the chain–chain correlation peak at intermediate q is still visible. The combination of those two signals enables describing the structure as a gel where proteins cross-link the PSS network.⁴ Macroscopically, the sample with $N = 625$ was a weakly turbid gel, whereas the samples with lower chain lengths were liquid and highly turbid.

In order to check whether the chain length is really a key parameter to shift from one structure to another, we have used a new chain length ($N = 800$) under the same conditions for the other parameters. Macroscopically, the sample is a weakly turbid gel. Both the scattering of lysozyme and PSS chains are plotted in Figure 1 together with the former data. Data for $N = 800$ are similar to the one previously observed for the $N = 625$ sample. In particular, one recovers the $q^{-2.5}$ decreasing law at low q values in the protein signal and the correlation peak of the PSS network chains in the PSS scattering. This confirms that we have two types of structure dense globules for short chains and cross-linked gel for long chains, as a function of the chain length, with a threshold between $N = 360$ and $N = 625$ for the concentrations and ionic strengths indicated above.

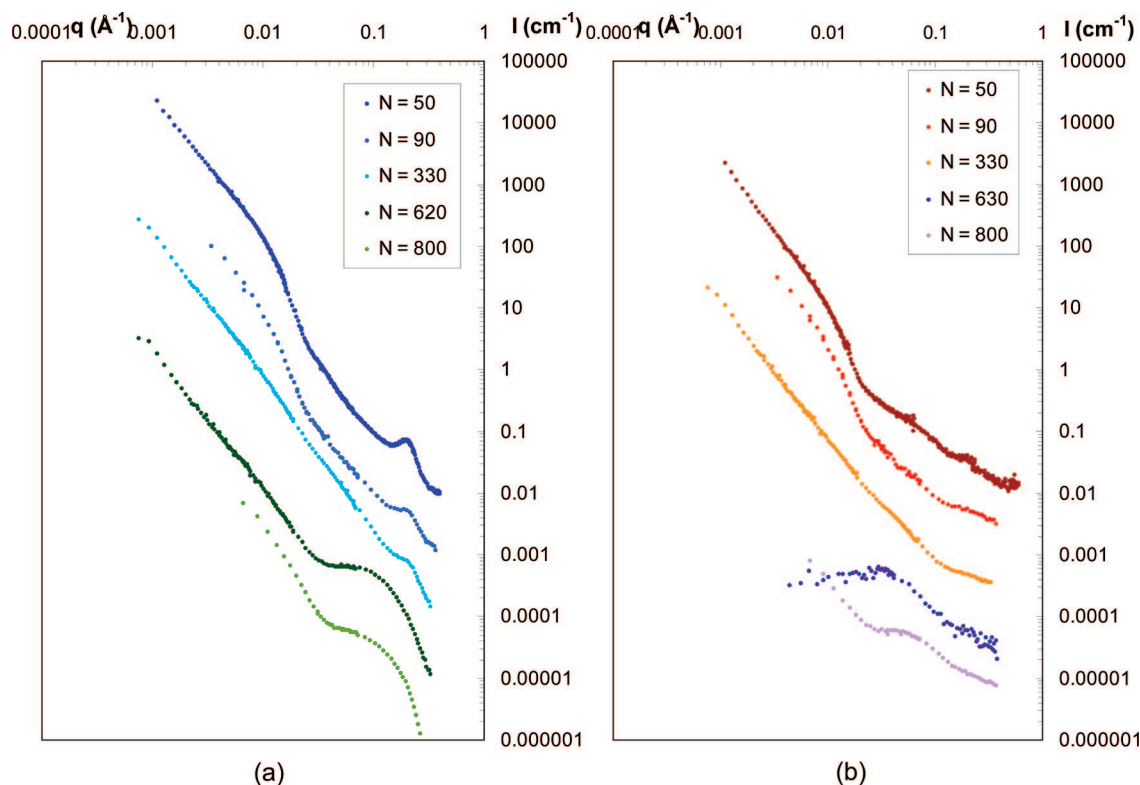


Figure 1. SANS spectra as a function of the PSS chain size for $[-]/[+]_{\text{intro}} = 3.33$ and $I = 5 \times 10^{-2}$ M. (a) Protein scattering: All of the curves are shifted from one to another by a decade for clarity. (b) PSS scattering: All of the curves are shifted from one to another by a decade for clarity. The spectra for $N = 90$, $N = 360$, and $N = 625$ have already been published in ref 4, and the spectra for $N = 50$ have already been published in ref 5. The error bars are smaller than the symbols.

1.b. Other Parameters. In order to determine whether this threshold depends on other parameters, we have then kept the PSS chains at $N = 800$ units, and varied the concentration in PSS, from 0.015 to 0.08 M (we also keep the protein concentration at 40 g/L and an ionic strength at $I = 5 \cdot 10^{-2}$ M). The complete series of SANS spectra can be found in Figure 7 in the Appendix, where it is compared with the 0.1 M sample measured formerly. $[-]/[+]_{\text{intro}}$ lies between 0.5 and 3.33. The collection of spectra signals gel above a PSS concentration $c_p = 0.08$ M and globules below 0.04 M. The transition, seen for 0.05 M, occurs on a narrow range.

Finally, a last parameter has been tuned, the ionic strength of the buffer, keeping fixed PSS chain length ($N = 800$) and species concentrations ($[-]/[+]_{\text{intro}} = 3.33$). Four samples have been made starting from 5×10^{-2} up to 5×10^{-1} M. The SANS spectra (Figure 8 in the Appendix) show that the two regimes can be reached when tuning the ionic strength, with a critical value clearly between 1×10^{-1} and 2×10^{-1} M (for this PSS chain length and species concentration).

2. Discussion on Threshold Values. What is driving the transition toward globules? Since the three parameters influencing the structure may affect the regime of dilution of the chains, let us revisit our idea that the two structures correspond to the dilute regime of the chains for the globules and to the semidilute regime of the chains for the gel. The threshold between those two regimes would then be set by the overlapping critical concentration of the chains, c^* . As noted in ref 4, the arrangement of the PSS chains in the gel structure is very close to the one of a pure solution of PSS chains in the semidilute region. The only observed difference lies in the mesh size of the network formed, which is larger in the presence of proteins, suggesting a local shrinking of the chains by the proteins: the q^* peak abscissa, corresponding to the network mesh size, is shifted toward low q in the presence of proteins.

To calculate the c^* value of a system of chains with the same wormlike conformation as in a pure PSS solution, we require the radius of gyration, R_g , of wormlike chains

$$R_g = \sqrt{2Ll_p} \quad (1)$$

where L is the length of the stretched chain and l_p is the persistence length. In the case of charged polymers such as PSS, l_p depends both on the intrinsic flexibility of the chain (10 \AA for PSS^{17,23,24}) and on electrostatic repulsions between monomers, which depend in turn on ionic strength.

The volume fraction of the solution occupied by the chains is then

$$\Phi = R_g^3 \times \frac{cN_a}{N} \quad (2)$$

where c is the monomeric concentration of the chains, N_a is the Avogadro number, and N is the number of monomers per chain. The critical concentration, c^* , between the semidiluted and diluted regimes is reached when the volume fraction is 1 when the chains begin to overlap and thus writes

$$c^* = \frac{N}{R_g^3 N_a} \quad (3)$$

The critical concentration finally depends on the number of monomers on the chain, N , and on the persistence length, l_p , only.

$$c^* = f\left(\frac{1}{N^{1/2}l_p^{3/2}}\right) \quad (4)$$

Let us now calculate c^* for our system and compare it to the experimental thresholds. For the case (Figure 7 in the Appendix) of a fixed chain length of $N = 800$, the fixed ionic strength of

$I = 50$ mM determines l_p for PSS chains alone in solution: the value is 50 \AA ¹⁷ (the counterions coming from PSS and proteins are taken into account in the ionic strength). This yields $c^* = 0.02$ M, which does not match our experimental threshold of 0.08 M. Similarly, if we take the example with variable chain length at fixed PSS concentration, 0.1 M, and ionic strength, $I = 50$ mM (data of Figure 1), we find, using the same formula and $l_p = 50 \text{ \AA}$, a chain length threshold of $N^* = 30$, which would put all of our samples in the semidiluted regime.

In summary, for the two cases, the c^* value of PSS chains calculated with the persistence length corresponding to pure PSS solutions does not match the gel–globule threshold. However, in the mixture, the chains interact with the proteins that bear opposite charges. A first effect was suggested by the shrinking of the PSS network (larger q^* observed in ref 4). In view of eq 4, the essential parameter is the persistence length, which could be modified after interaction of PSS with the proteins. By measuring the conformation of the PSS chains inside the complexes, it will be possible to determine if it is still wormlike, and to obtain a new value of the persistence length in the presence of proteins in order to calculate a new critical concentration, c^* .

IV. The Conformation of the PSS Chains

In order to get the conformation of the PSS chains inside the complexes in a SANS experiment, one needs to separate in the scattering signal their form factor from the strong interchain structure factor arising from the electrostatic repulsions between the chains. The first solution to be imagined is to work in very low concentrations to weaken as much as possible the structure factor. However, changing the dilution would act on the conformation of the chains and the measurement would be senseless. A tricky method is thus required to get rid of interchain scattering, and keep only intrachain contribution. The method we chose consists of making a set of several different samples with the same total chain concentration but different fractions of deuterated and non-deuterated chains in a solvent matching the scattering length density of hydrogenated chains. When the amount of deuterated chains tends to zero, the system tends to behave as a set of single PSS chain from a scattering point of view, thanks to the hiding of the hydrogenated chains. However, at the same time, the interactions between the chains in the system do not change because the total concentration of chains remains identical. The principle is recalled in the sketch of Figure 2a that shows a system of pure PSS chains in the semidilute regime for the four ratios of deuterated chains we chose (25, 50, 75, and 100%) in a H_2O solvent (upper sketch) and in a 57%/43% $\text{H}_2\text{O}/\text{D}_2\text{O}$ solvent (lower sketch) that matches the hydrogenated chains. In general, this method would not apply for chains within complexes because the protein scattering would remain. Here comes the great advantage of our system: the neutron density length of lysozyme is equal to the one of the hydrogenated PSS! Thus, both species can be matched simultaneously and the measurement of conformation can be done also in the presence of proteins (see the sketch of Figure 2b).

For pure solutions of PSS chains, since we have now two kinds of PSS chains, hydrogenated ones and deuterated ones, mixed in the solution, the total scattering takes into account the correlations between chains of the same kind and chains of different kind:

$$I(\vec{q}) = \frac{1}{V} \left\langle \sum_{ij} k_i k_j \exp(i\vec{q}(\vec{r}_i - \vec{r}_j)) \right\rangle \quad (5)$$

where k_i (cm or \AA) = $b_i - b_s$ ($V_{\text{mol},i}/V_{\text{mol},s}$) is the “contrast length” between one repeating unit of scattering length b_i and molar volume $V_{\text{mol},i}$ and a solvent molecule (b_s , $V_{\text{mol},s}$).

Let us assume first that all chains are labeled in the same way with respect to solvent; i.e., for all i , we have $k_i = k_A$. The concentration is c_p , in mol/L (or mol/Å³), so the total volume fraction of chains is $\Phi_T = N_A c_p V_{\text{mol},i}$, where N_A is the Avogadro number.

$$I(q) \text{ (cm}^{-1} \text{ or } \text{\AA}^{-1}) = (1/V) \quad d\Sigma/d\omega = k_A S_{\text{TAA}}(q) \quad (6)$$

Using Å and Å⁻¹ as the units for k_H and $I(q)$, we obtain $S_{\text{TAA}}(q)$ in Å⁻³. Quite generally,

$$S_{\text{TAA}}(q) = S_{\text{TAA}}(q) + S_{2\text{AA}}(q) \quad (7a)$$

where

$$S_{1\text{AA}}(q) \text{ (}\text{\AA}^{-3}\text{)} = \left\langle \sum_{\alpha \text{ with } \beta=\alpha} \sum_{i,j} \exp(i\vec{q}(\vec{r}_i^\alpha - \vec{r}_j^\beta)) \right\rangle \quad (7b)$$

corresponds to the correlations between monomers i,j of the same chain $\alpha = \beta$ (intrachain scattering), and

$$S_{2\text{AA}}(q) \text{ (}\text{\AA}^{-3}\text{)} = \frac{1}{V} \left\langle \sum_{\alpha, \beta \neq \alpha} \sum_{i,j} \exp(i\vec{q}(\vec{r}_i^\alpha - \vec{r}_j^\beta)) \right\rangle \quad (7c)$$

corresponds to the correlations between monomers i,j of two different chains α and $\beta \neq \alpha$ (interchain scattering).

Assume now that chains are labeled in two different ways. In practice, we use a mixture of d-PSS chains ($k_i = k_D$) and h-PSS chains ($k_i = k_H$). The scattered intensity becomes

$$I(q) \text{ (cm}^{-1}\text{)} = (1/V) \quad d\Sigma/d\Omega = k_H^2 S_{\text{HH}}(q) + 2k_H k_D S_{\text{HD}}(q) + k_D^2 S_{\text{DD}}(q) \quad (8)$$

where $S_{\text{HH}}(q)$ is the scattering of the hydrogenated chains, $S_{\text{DD}}(q)$ is the scattering of the deuterated chains, and $S_{\text{HD}}(q)$ is the cross-term. In a solvent that matches the scattering length density of the hydrogenated chains, $k_H = 0$; hence,

$$I(q) \text{ (cm}^{-1}\text{)} = (1/V) \quad d\Sigma/d\omega = k_D^2 S_{\text{DD}}(q) \quad (9)$$

The total volume fraction of chains in the solution is the sum of the volume fractions of the two types of chains, $\Phi_T = \Phi_H + \Phi_D$. Since H and D chains are perfectly identical except for the value of b (in particular $V_{\text{molH}} = V_{\text{molD}} = V_{\text{mol}}$), we can write

$$S_{\text{DD}}(q) = \phi_D S_1(q) + \phi_D^2 S_2(q) \quad (10)$$

with $S_1(q)$ and $S_2(q)$ concerning all H and D chains being defined as above by eqs 7b and c. Eventually,

$$I(q) \text{ (cm}^{-1}\text{)}/\phi_D = k_D^2 (S_1(q) + \phi_D S_2(q)) \quad (11)$$

If we add now lysozyme in the system, numerous new correlation terms are to be taken into account! However, in the 57%/43% H₂O/D₂O solvent that matches here also the protein

neutron density length (as well as the hydrogenated chains), all terms with k_H in the front factor vanish, a huge simplification which makes eq 11 still valid.

Experimentally, we will measure, for a given system, the scattering for four [PSS_d]/[PSS_h] ratios. For each q value, the four intensities will be linear as a function of Φ , and the extrapolation to $\Phi = 0$ will provide the value of S_{1D} . The dimensionless form factor of the PSS chains, $P(q)$ ($\lim_{q \rightarrow 0} P(q) = 1$), will finally be obtained from $S_1(q)$:

$$\lim_{\phi_D \rightarrow 0} I(q)/(\phi_D k_D^2) = S_1(q) \text{ (}\text{\AA}^{-3}\text{)} = (1/V_{\text{mol}}) N_w P(q) \quad (12)$$

at each q value probed in the experiment.

In the following section, we describe three measurements of PSS form factors, one for a solution of pure PSS chains and two for solutions of PSS chains complexed with proteins in the gel-like structure and in the globular structure.

1. Results. 1.1. Pure PSS Solutions. We have first determined the conformation of the PSS chains alone in solution to check whether we find with this method of measurement the value of the persistence length given in the literature (which was actually obtained for the first time with the same method²⁴). We use a solution of PSS at 0.1 M, which corresponds to the concentration we will use to determine the conformation inside the complexes, and a buffer ionic strength of 5×10^{-2} mol/L. The rate of deuterated chains, Φ_d ([PSS_d]/[PSS_h]), is set to 25, 50, 75, and 100%. Figure 3 shows all of the scattering spectra renormalized by Φ_d to enable a direct comparison between the signals.

For high q values ($q > 0.05 \text{ \AA}^{-1}$), the four signals are equivalent, but at low q values, they become sensitive to the structure factor. In this low q region, one gets a correlation peak due to the strong electrostatic repulsions between the chains. At q tending toward zero, the structure factor decreases to values much lower than 1. The contribution of the correlation peak on the scattering progressively vanishes when the amount of deuterated chains decreases, and the signal progressively tends to the signal of one chain. The extrapolation at $\Phi_d = 0$ at each q value as explained before is represented in red in Figure 3.³¹ At low q , it is thus higher than all of the measured ones. At high q , it is similar to the experimental scattering signal values ($q > 0.05 \text{ \AA}^{-1}$) because, in this q region, the structure factor is very close to 1. The extrapolated intrachain scattering is presented in a Kratky plot ($Iq^2 = f(q)$, linear axes, q range from $q = 10^{-3}$ to $q = 6 \times 10^{-2}$) in Figure 4, which enables a good comparison of the experimental signal with the calculated scattering of a wormlike chain.³²

In this model, the wormlike chain has a constant curvature characterized by a persistence length, l_p , characterized as follows.

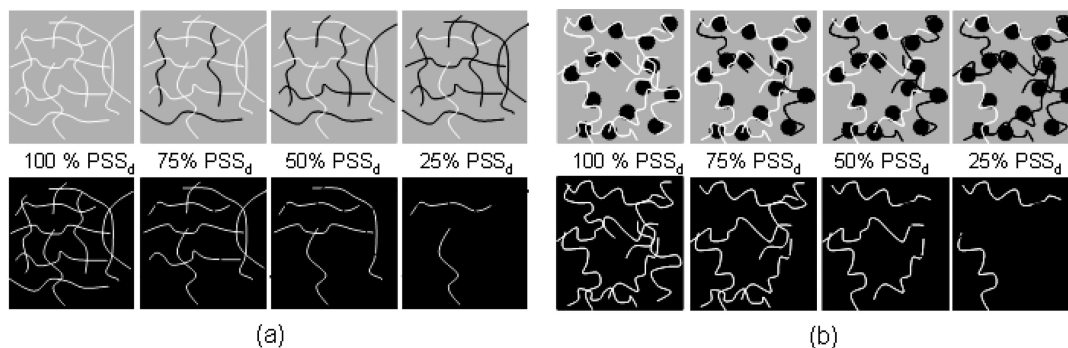


Figure 2. Principle of the measurement of the form factor of a PSS chain by contrast matching in a SANS experiment: (a) measurement in pure solutions of PSS chains; (b) measurement in complexes made with lysozyme. The total amount of PSS chains is constant for all samples. For each drawing, lysozyme and PSS_h chains are both in black and PSS_d chains are in white, either in 100% H₂O solvent (grey, upper sketch) or in a 57% H₂O/43% D₂O solvent (black, lower sketch).

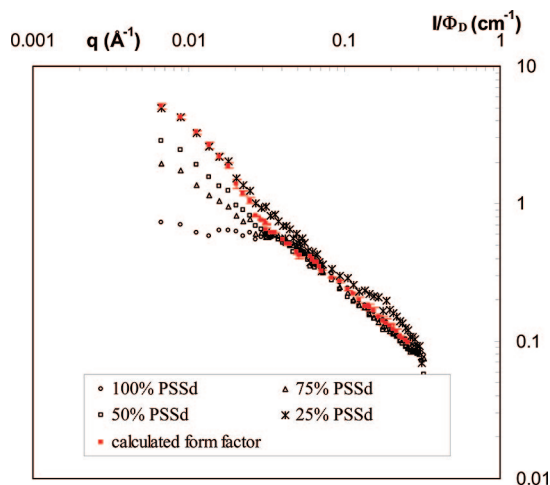


Figure 3. Conformation of a PSS chain in pure solutions of PSS chains ([PSS] = 0.1 M, $I = 5 \times 10^{-2}$ M). SANS spectra for the four ratios of deuterated chains in a 57%/43% H₂O/D₂O solvent (open symbols) and extrapolation of the PSS form factor (red filled squares). The error bars for the experimental data are smaller than the symbols.

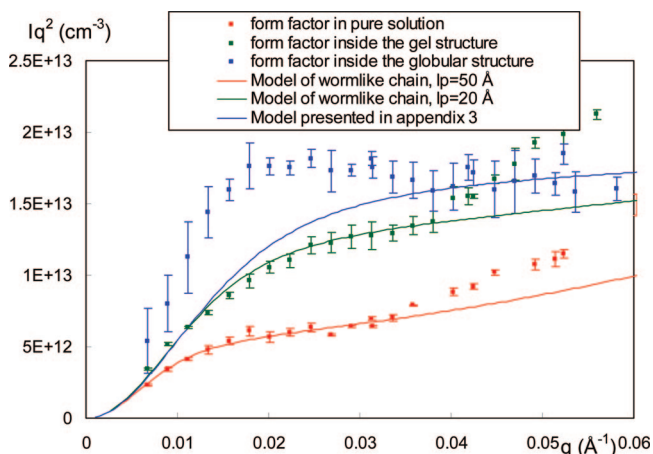


Figure 4. Kratky plot of the three PSS form factors: pure solution of PSS (red squares); PSS chains inside the gel structure at $I = 5 \times 10^{-2}$ M (green squares); PSS chains inside the globular structure at $I = 5 \times 10^{-1}$ M (blue squares). The continuous lines correspond to the fits. Red line: form factor of a wormlike chain ($l_p = 50$ Å). Green line: form factor of a wormlike chain ($l_p = 20$ Å). Blue line: model of a linear combination of a factor of Gaussian chains with an effective gyration radius of 85 Å and of a wormlike chain ($l_p = 30$ Å). See Appendix 3 for details of the third model.

If Ψ is the angle between the tangents of two points of the chains separated by a distance, l , then

$$\langle \cos(\Psi) \rangle \approx \exp(-l/l_p) \quad (13)$$

Sharp and Bloomfield³³ have given the following expression for the form factor $P(q)$ of wormlike chains that takes into account the finite size of chains of length L , at low q :

$$P(q) = \frac{2(\exp(-x) + x - 1)}{x^2} + \left[\frac{4}{15} + \frac{7}{15x} - \left(\frac{11}{15} + \frac{7}{15x} \right) \exp(-x) \right] \frac{2l_p}{L} \quad \text{for } qL_p < 4 \quad (14)$$

with $x = Lq^2 l_p / 3$. This expression is valid until $qL_p < 4$. It enables us to fit all the parts of the signal at the lower q values. When $qL_p > 4$, then the signal follows an asymptotic law of Des Cloizeaux:³⁴

$$P(q) = \frac{\pi}{qL} + \frac{2}{3q^2 l_p} \quad (15)$$

The molecular weight distributions in our measurements (in other words the chain length, L) are known. The extrapolated spectrum is here in absolute intensities (cm⁻¹), and we calculate the volume fraction, ϕ_D , of the chains from their molar volume, V_{mol} , their concentration (0.1 M), and the neutronic contrast ($\Delta\rho^2 = k_D^2/V_{\text{mol}}^2 = 1.49 \times 10^{21}$ cm⁻⁴). The low q value enables checking that one recovers the molecular weight, N_w , of the PSS chains.³⁵ The only one parameter that can be tuned to fit the experimental signal is the persistence length, l_p . In pure polyelectrolyte solutions with monovalent cations, this parameter depends on the intrinsic backbone persistence length, l_{p0} , and on electrostatic repulsions between charged monomers (for a flexible backbone like PSS, l_{p0} here is small (10 Å), and the perturbation-like additivity law proposed by Odijk³⁶ could not be verified). In Figure 3 is represented the best fit using eqs 12 and 13, yielding an l_p value of 50 Å, equal to values formerly published for the same ionic strength^{17,24}

1.2. PSS inside the Gel Structure. The pure solution case being successful, we have used the same protocol with a PSS/lysozyme mixture in the gel regime. The concentration of PSS is 0.1 M, the concentration of lysozyme is 40 g/L, which leads to an introduced charge ratio $[-]/[+]_{\text{intro}}$ of 3.33. The buffer ionic strength is 5×10^{-2} mol/L. A macroscopic gel is obtained for every sample. The amount of deuterated and hydrogenated chains does thus not affect the structure. In Figure 5 are represented the four PSS signals for $\Phi_d = 25, 50, 75$, and 100% as well as the extrapolated form factor.³¹

The signals obtained at the different ϕ_D values are very close to the ones of pure PSS solutions. The main differences are the position of the polyelectrolyte peak which is shifted toward the lower q and a slight upturn at low q . The slight upturn is probably due to small heterogeneities in the network of PSS chains. The shift of the peak was observed formerly⁴ and attributed to a shrinking of the PSS network mesh. Like in the case of PSS chains alone, it vanishes when Φ_d tends to 0 and disappears in the extrapolated signal at $\Phi_d = 0$, shown in green in Figure 5. The latter is also plotted in a Kratky representation in Figure 4, for comparison with the signal of pure PSS solution at the same concentration. In the gel structure, PSS chains still display a wormlike behavior, but their persistence length has

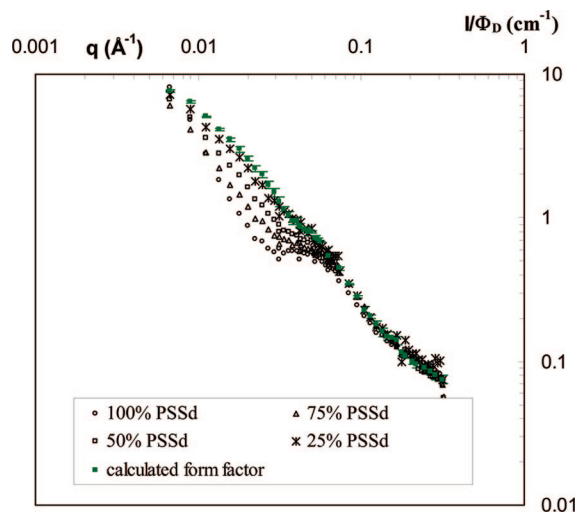


Figure 5. Conformation of a PSS chain in complexes with a gel-like structure. ([Lyso] = 40 g/L, [PSS] = 0.1 M, $I = 5 \times 10^{-2}$ M). SANS spectra for the four ratios of deuterated chains in a 57%/43% H₂O/D₂O solvent (open symbols) and extrapolation of the PSS form factor for the PSS inside the complexes (green filled squares). The error bars for the experimental data are smaller than the symbols.

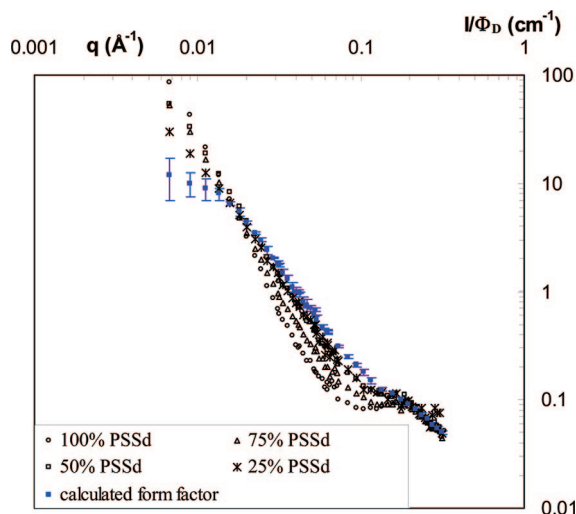


Figure 6. Conformation of a PSS chain in complexes with a globular structure. ([Lyso] = 40 g/L, [PSS] = 0.1 M, $I = 5 \times 10^{-1}$ M). SANS spectra for the four ratios of deuterated chains in a 57%/43% H₂O/D₂O solvent (open symbols) and extrapolation of the PSS form factor for the PSS inside the complexes (blue filled squares). The error bars for the experimental data are smaller than the symbols.

changed, as obvious from the following: (1) the different q value for the upturn of the plateau appearing in the Kratky plot: The upturn position is at $q = 0.025 \text{ Å}^{-1}$ for the PSS inside the complexes when it is at $q = 0.015 \text{ Å}^{-1}$ for the PSS alone. (2) as well as from the different ordinate of this plateau: $1.2 \times 10^{-19} \text{ cm}^{-3}$ for the PSS inside the complexes, whereas it is $5 \times 10^{-20} \text{ cm}^{-3}$ for the PSS alone.

These strong changes indicate that the persistence length has decreased. The same conclusion can be drawn from a fit to a wormlike chain, yielding $l_p = 20 \text{ Å}$ instead of 50 Å for pure PSS solutions. The chains are shrunk.

1.3. PSS inside the Globular Structure. Finally, we have determined the intrachain scattering of PSS inside the globular complexes. For a direct comparison with the two other cases, we used the same chain and lysozyme concentrations ([PSS] = 0.1 M, [lysozyme] = 40 g/L). In order to force the structure to be globular, we increased the ionic strength of the buffer to 0.5 M, on the basis of results of Figure 7 in the Appendix. The four PSS signals for $\Phi_d = 25, 50, 75$, and 100% as well as the extrapolated intrachain scattering are represented in Figure 6.³¹

This time, all signals are very different from the ones from pure PSS solutions. First, the scattering of the 100% deuterated sample, which indeed is the scattering from polymer only, as already seen in Figure 1: whereas at high q values it still decays with a typical q^{-1} decreasing law, at slightly lower q , a peak at 0.2 Å^{-1} due to the contact of the proteins is present here. This correlation is clearly seen in globular complexes for the protein–protein signal, but it is here also seen in the PSS–PSS scattering. At smaller q , the scattering decays like q^{-4} ; this is the surface scattering of the large dense globules (radius larger than 300 Å).

If we look now at the different samples with lower deuteration rates, these two features (the peak at 0.2 Å^{-1} and the q^{-4} intermediate behavior) are progressively vanishing because they are both linked to the structure factor. Hence, unlike the two precedent cases, the intensity of the signal at low q values is higher in the presence of the structure factor: interactions are here no longer repulsive but attractive, since PSS chains are aggregated within the globules. When the deuteration rate tends to zero, the low q intensity tends toward the scattering of one chain, and thus decreases. Note that all of the different signals cross at the same abscissa, $q = 0.02 \text{ Å}^{-1}$. This means that the

structure factor is null for this wave vector, so we get a direct measurement of the absolute intensity of the form factor for any Φ_d . At high q values, the $\Phi_d = 0$ extrapolated intrachain scattering is close to the signals of pure PSS and PSS inside the gel structure: it scatters like q^{-1} , with a crossover when going toward low q values.

This intrachain scattering factor is compared in Figure 4 with the form factor of the pure PSS determined previously in a Kratky plot. In this representation, it is possible to see immediately that the conformation adopted by the PSS chains inside the dense complexes is completely different from the two previous ones. Chains are no longer wormlike. Instead, $q^2 I(q)$ displays a slight maximum around 0.025 Å^{-1} followed at larger q by a plateau.

This $q^2 I(q)$ plateau suggests a q^{-2} scattering behavior showing chains close to a Gaussian behavior, following a random walk inside the globules. The simplest model to be imagined to fit the plateau is a Debye function corresponding to the form factor of a Gaussian chain with the gyration radius of the PSS chain (57 Å for $N = 800$). Such a calculated curve (not shown here) would be very different from the experimental one because the plateau would start around 0.05 Å^{-1} instead of 0.02 Å^{-1} here, and its ordinate would be $\sim 4 \times 10^{-19} \text{ cm}^{-3}$ instead of $1.5 \times 10^{-19} \text{ cm}^{-3}$ here. This is in accordance with the fact that the inner volume of the globules is not fully accessible to the chains because of the presence of the proteins. The chains have thus an effective gyration radius higher than the one of a pure Gaussian chain. Moreover, a part of the chains would be located in a PSS shell around the globules.

A calculation of a form factor corresponding to a linear combination of a fraction of chains in the Gaussian state with the effective radius and a fraction of PSS wormlike chains is presented in Appendix 3. The effective radius of gyration is estimated by calculating the number of proteins complexed per chain. This enables us to fit correctly the value of the plateau in absolute scale (see Figure 4) at large q but not the onset of the plateau (0.02 Å^{-1}) or the smooth maximum. One may wonder whether this maximum is linked to the size of the globules: this is not the case, since it would give for the globules a radius of 250 Å , much lower than their mean radius which is at least 300 Å for a salinity buffer of 0.5 M , as extracted from the PSS–PSS or protein–protein signal (these scatterings—Figure 7 in the Appendix—still vary like q^{-4} at $q = 0.0035 \text{ Å}^{-1}$, i.e., $R > 1/0.0035 \text{ Å} > 300 \text{ Å}$).

An alternative could be found in a third type of combination, between wormlike chains and spheres: the maximum in the $q^2 S_1(q)$ chain signals at large scale a globular shape, while at short scales (at large q) it is not very different from a rodlike behavior (in practice, it smoothly crosses the wormlike chain signal). Such a combination was found for partially sulfonated PSS chains, when some of the units are hydrophobic (like polystyrene). In this case, the pearl necklace structure predicted by Dobrynin and Rubinstein³⁷ was observed.²⁹ In the case studied now, our maximum is at 10 times lower q , corresponding to spheres larger than 100 Å , but again, as said just above, they are somewhat too small compared to the globule size, as extracted from the PSS–PSS or protein–protein signal. Please also note that the complexation between both components still occurs at large salinities, contrary to the release of proteins at high I suggested by simulations^{19,21}

V. Discussion

1. Values of c^* and Gel–Globule Threshold. The measurement of the conformation of the PSS chains within the gelled samples shows that the interactions between the proteins and the polyelectrolyte leads to the shrinking of the PSS chains, as we suggested in ref 4, because the persistence length of the

chains is strongly reduced, from 50 Å in pure PSS chain solution down to 20 Å in the presence of proteins. Please note that this value of 20 Å is likely to be an average value. Some chain parts, not linked, could keep their genuine 50 Å persistence length, which suggests that, for other parts, l_p would be even shorter (the minimum is the intrinsic value 10 Å).

Let us make use of this new value of the persistence length to test if the transition between the two regimes (gel structure or dense globular structure) can be the transition from the dilute regime of the chains to the semidilute one. We recalculate the overlapping concentration of the chains, with $l_p = 20$ Å. From eq 4, the critical chain polymerization degree for the dilute to semidilute crossover at unit concentration 0.1 M (and $I = 50$ mM) is $N^* = 500$. This new value perfectly matches the gel-to-globule experimental threshold, $360 < N^* < 625$ (see Figure 1).

We can also recalculate c^* for a given chain length at a fixed ionic strength. We obtain $c^* = 0.08$ M for $N = 800$ monomers at $I = 50$ mM, which also perfectly matches the gel–globule threshold found by SANS in Appendix 2. This value of c^* is also very close to 0.1 M, the chain concentration of the samples for which the buffer ionic strength was tuned in Appendix 1, where the transition appears for I between 100 and 200 mM. From eq 4, at these chain concentrations and lengths, we obtain for a transition between 100 and 200 mM $l_p^* = 17$ Å, a value lower by 3 Å when passing from 50 to 150 mM.

In summary, the calculation of c^* with the new value of the persistence length, whatever the parameter tuned (PSS chain length, PSS concentration, ionic strength), strongly confirms that the dilution regime of the PSS chains is the key factor for the transition between the “gel” structure and the globular structure.

2. Chain Conformations. A closer look at the conformation of the PSS chains enables us to understand how the two structures are formed. In the gelled samples, after interaction with the proteins, the key point is that some parts of chains remain wormlike. The form factor shape is compatible with a combination of two conformations. This suggests that some parts of the chains are not complexed with the lysozyme and remain free in solution. For the samples studied in part IV (average l_p value of 20 Å), a simple calculation gives 75% of the chains collapsed on proteins (with $l_p = 10$ Å) and 25% free in solutions (with $l_p = 50$ Å). For $[PSS] = 0.1$ M, this gives 0.025 M of free chains, still higher than c^* for $l_p = 50$ Å when the chains are long enough (0.02 M for $N = 800$ and 0.022 M for $N = 600$). The free chains can thus still form the same transient network as in pure PSS solutions. The transient network of the free PSS sequences is thus cross-linked by the chain sequences bound to lysozyme.

For the globular samples, the complexation can be considered as a two-step process. An initial complexation of the chains with the proteins leaves 25% of the chains free for $[PSS] = 0.1$ M and $[lysozyme] = 40$ g/L. When the concentration of these free chains is too dilute to form a network (ones gets for example a c^* value of 0.031 M for $N = 360$ to compare to a concentration of free chains of 0.025 M), the system collapses to form the globular structure due to the electrostatic interactions between species of opposite charge and the gain of entropy associated with the release of counterions.⁶ In such a structure, the core of the globules is very dense and electrically neutral, suggesting a local interaction of all PSS units with a positive charge of lysozyme.⁵ The PSS chains are thus strongly confined by proteins and cannot thus adopt a wormlike behavior anymore. In the q^2I plot, the slight maximum may be due to a spherically collapsed global shape, while the plateau observed at large q suggests that the inner conformation is not far from a random walk inside an effective volume fixed by the number of proteins interacting with the chain (see Appendix 3).

VI. Conclusion

We have shown that the transition between the two main structures of PSS/lysozyme complexes, aggregated globules and gel, corresponds to chain overlapping. Prior to this, we have to account for a first stage where chain spatial expanse is reduced by interaction with the proteins. The consecutive concentration threshold, c^* , can then be tuned by usual parameters: chain length, tuning of the persistence length by the salinity of the buffer. The control of the transition is especially important for tuning properties such as rheology, response to dilution, or access to enzymatic sites for applications in pharmacology or biosensors.

This conclusion is made possible by the measurement of the form factor of chains within the complexes. We describe the chain conformation as wormlike and semiflexible; we extract a persistence length, and we show that it decreases in the presence of proteins after electrostatic attractions between species. To our best knowledge, this is the first form factor measurement for a polymer in a mixed system of two interacting species in aqueous solutions. It is based on a small angle neutron scattering method, which is powerful but sophisticated: it requires two different labeled versions of the polymer (here hydrogenated and deuterated PSS) and that the second component of the mixture has the same neutron scattering length density as one of the labeled versions of the polymer (here lysozyme and hydrogenated PSS). Obviously, this is not always possible in complexes, and therefore seems demanding. However, many components encountered in soft matter have similar neutron scattering length densities in their hydrogenated version and most common polymers are available in deuterated versions; therefore, we would like to point out that this method may apply to other systems.

Appendix 1: SANS Determination of the Gel–Globule Threshold When the PSS Chain Concentration Is Varied

In this series of experiments, six samples have been prepared with the same amount of protein (40 g/L) at a fixed ionic strength of $I = 5 \times 10^{-2}$ M in a 100% D₂O solvent (matching of the PSS scattering). The concentration of deuterated PSS chains has been varied from 0.015 to 0.08 M to determine the threshold between the gel regime and the globular regime as a function of the concentration of PSS chains.

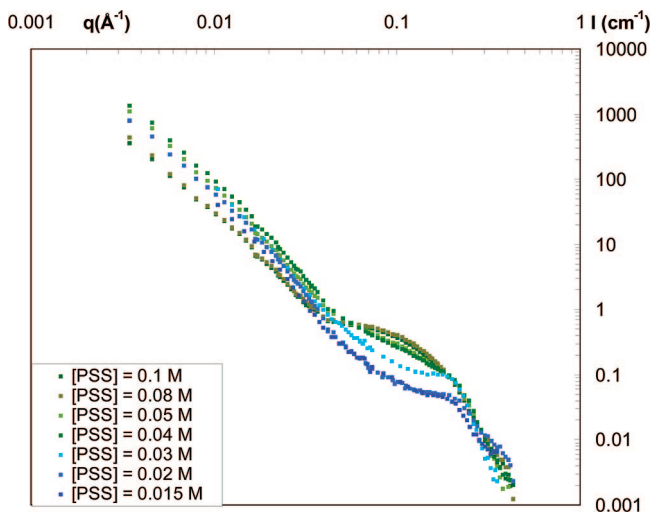


Figure 7. SANS spectra as a function of the concentration of PSS chains for a concentration in protein of 40 g/L in a 100% D₂O buffer (protein signal) at a fixed ionic strength of $I = 5 \times 10^{-2}$ M (protein scattering). For the two lowest concentrations of PSS, the signal coming from free proteins has been subtracted (see ref 5 for full details). The error bars are smaller than the symbols.

The spectra are compared in Figure 7 to the one of the sample at PSS = 0.1 M (see Figure 1). For the highest concentrations of PSS chains (0.08 and 0.1 M), the structure formed is the gel (the scattering spectra show the typical $q^{-2.5}$ decay behavior at low q and the absence of correlation peak at high q). Then, for lower concentrations, the scattering decay at low q progressively shifts from a $q^{-2.5}$ behavior to a q^{-4} one for the lowest concentrations in PSS chains while the characteristic correlation peak at $q = 0.2 \text{ \AA}^{-1}$ of the globular regime begins to appear. The threshold between the gel and the globular structure can therefore be defined to be at a concentration of PSS chains of 0.08 M.

Appendix 2: SANS Determination of the Gel–Globule Threshold When the Ionic Strength Is Varied

In this series of experiments, four samples have been prepared with the same amount of protein (40 g/L) and of deuterated PSS chains (0.1 M) in a 100% D₂O solvent (matching of the PSS scattering). The ionic strength has been varied from $I = 5 \times 10^{-2}$ to $I = 5 \times 10^{-1}$ M to determine the threshold between the gel regime and the globular regime as a function of the ionic strength.

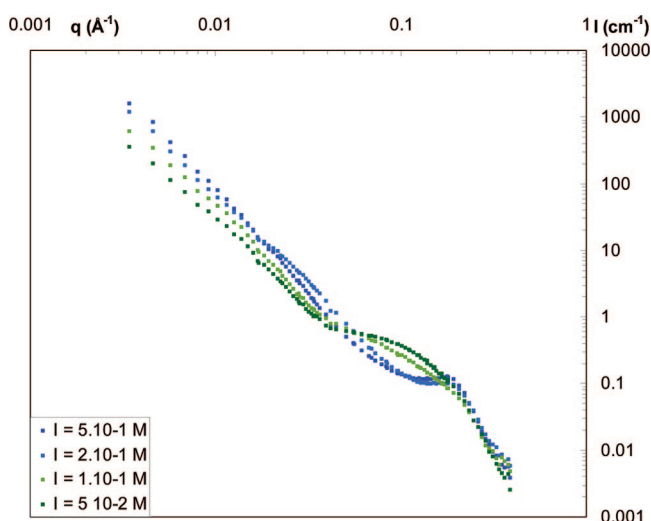


Figure 8. SANS spectra as a function of the ionic strength at a fixed concentration in PSS chains of 0.1 M and in protein of 40 g/L in a 100% D₂O buffer (protein scattering). The error bars are smaller than the symbols.

The spectra presented in Figure 8 show the two different behaviors depicted in section III.1 for the two lowest and the two highest ionic strengths. For the two highest ionic strengths, we recover the typical features of the globules (the correlation peak at 0.2 \AA^{-1} and the q^{-4} scattering decay at intermediate q) and the typical features of the gel for the two lowest ionic strengths (the $q^{-2.5}$ scattering decay at low q). The threshold between the gel and the globular structure can therefore be defined in the following range of ionic strength: $1 \times 10^{-1} < I < 2 \times 10^{-1}$ M.

Appendix 3: Attempt of Adjustment of the PSS Form Factor Signal in the Globular Structure

In order to adjust the signal of the PSS chains inside the dense globules, we have assumed that the chains have a Gaussian-like behavior with an effective gyration radius inside the complexes fixed by volume occupied by the number of proteins interacting with one chain. This radius is the main parameter of the model. First of all, we estimate the number of proteins, N , interacting with a chain with the number of monomer, N_{mono} . The inner charge ratio within the globules $[-]/[+]_{\text{inner}}$ can be

determined by the ratio of the PSS signal to the protein signal intensities, $I_{\text{PSS}}/I_{\text{lyso}}$ at low q values (the full method is explained in ref 5). This value is estimated to be around 2.5 for the chain with 800 monomers at 0.5 M (the lysozyme spectra are given in Figure 8 and the PSS spectra in Figure 5). As each PSS monomer bears a negative charge, we get

$$N = \frac{N_{\text{mono}}}{Z_{\text{lyso}}[-]/[+]_{\text{inner}}} \quad (\text{A.1})$$

with Z_{lyso} being the net charge of lysozyme. For the chain considered here, the number of proteins, N , is 30. The associated volume occupied is then dependent on the protein compactness:

$$V_{\text{occup}} = \frac{NV_{\text{lyso}}}{\Phi_{\text{inner_lyso}}} \quad (\text{A.2})$$

where V_{lyso} is the volume of lysozyme and $\Phi_{\text{inner_lyso}}$ is the volume fraction of the proteins within the globules. This latter can be evaluated from the lysozyme scattering modelization (the full method is explained in ref 5) and is 0.15. The effective gyration radius of confinement of a chain can then be directly calculated:

$$R_g = \sqrt[3]{\frac{3V_{\text{occup}}}{4\pi}} \quad (\text{A.3})$$

The value obtained is 85 \AA . We consider that the chain has a Gaussian-like behavior within this effective gyration radius. The form factor of the chain is thus a Debye function:

$$P(q) = \frac{2(e^{-X} - 1 + X)}{X^2} \quad \text{with} \quad X = q^2 R_g^2 \quad (\text{A.4})$$

In the globular regime, we showed in ref 5 that the globules are surrounded by a shell layer coexisting with free chains when $[-]/[+]_{\text{intro}} = 3.33$. In order to take into account the signal of these free chains, we have considered that they have a standard wormlike chain behavior with the persistence length of pure solutions of PSS chains. For this high ionic strength (0.5 M), l_p is 30 \AA .¹³ The final form factor result is a linear combination of signals of Gaussian chains and wormlike chains taking into account the amount of free chains. This amount of free chains has been calculated from the inner charge ratio, $[-]/[+]_{\text{inner}}$, and is of 23%.

References and Notes

- (1) Tribet, C. *Physical chemistry of polyelectrolytes*; Radeva, T., Ed.; Surfactant Science Series; M. Dekker: New York, **1999**; Chapter 19, pp 687–741.
- (2) Cooper, C. L.; Dubin, P. L.; Kayitmazer, A. B.; Turksen, S. *Curr. Opin. Colloid Interface Sci.* **2005**, *10*, 52–78.
- (3) Turgeon, S. L.; Schmitt, C.; Sanchez, C. *Curr. Opin. Colloid Interface Sci.* **2007**, *12*, 166–178.
- (4) Cousin, F.; Gummel, J.; Ung, D.; Boué, F. *Langmuir* **2005**, *21*, 9675–9688.
- (5) Gummel, J.; Demé, B.; Boué, F.; Cousin, F. *J. Phys. Chem. B* **2006**, *110*, 24837–24846.
- (6) Gummel, J.; Cousin, F.; Boué, F. *J. Am. Chem. Soc.* **2007**, *129* (18), 5806–5807.
- (7) Gummel, J.; Cousin, F.; Verbavatz, J. M.; Boué, F. *J. Phys. Chem. B* **2007**, *111* (29), 8540–8546.
- (8) Bohidar, H.; Dubin, P. L.; Majhi, P. R.; Tribet, C.; Jaeger, W. *Biomacromolecules* **2005**, *6*, 1573–1585.
- (9) Borrega, R.; Tribet, C.; Audebert, R. *Macromolecules* **1999**, *32*, 7798–7806.
- (10) Xia, J.; Dubin, P. L.; Kim, Y.; Muhoberac, B. B.; Klimkowski, V. J.; Valentine, J. J. *J. Phys. Chem. B* **1993**, *97* (17), 4528–4534.
- (11) Park, J. M.; Muhoberac, B. B.; Dubin, P. L.; Xia, J. *Macromolecules* **1992**, *25*, 290–295.
- (12) Ball, V.; Winterhalter, M.; Schwinte, P.; Lavallo, P.; Voegel, J. C.; Schaaf, P. *J. Phys. Chem. B* **2002**, *106*, 2357–2364.
- (13) Berret, J.-F.; Hervé, P.; Aguerre-Chariol, O.; Oberdisse, J. *J. Phys. Chem. B* **2003**, *107* (32), 8111–8118.

- (14) Berret, J.-F.; Vigolo, B.; Eng, R.; Herve, P.; Grillo, I.; Yang, L. *Macromolecules* **2004**, *37* (13), 4922–4930.
- (15) Trabelsi, S.; Guillota, S.; Ritacco, H.; Boué, F.; Langevin, D. *Eur. Phys. J. E* **2007**, *23* (3), 305–311.
- (16) Berret, J.-F.; Schonbeck, N.; Gazeau, F.; El Kharrat, D.; Sandre, O.; Vacher, A.; Airiau, M. *J. Am. Chem. Soc.* **2006**, *128* (5), 1755–1761.
- (17) Spiteri, M. N.; Boué, F.; Lapp, A.; Cotton, J. P. *Phys. Rev. Lett.* **1996**, *77* (26), 5218–5220.
- (18) Litmanovich, E. A.; Zakharchenko, S. O.; Stoichev, G. V. *J. Phys. Chem. B* **2007**, *111*, 8567–8571.
- (19) Ulrich, S.; Seijo, M.; Stoll, S. *Curr. Opin. Colloid Interface Sci.* **2006**, *11* (5), 268–272.
- (20) Skepö, M.; Linse, P. *Phys. Rev. E* **2002**, *66*, 051807.
- (21) Stoll, S.; Chodanowski, P. *Macromolecules* **2002**, *35*, 9556–9562.
- (22) Kayitzamer, A. B.; Seyrek, E.; Dubin, P. L.; Staggemeier, B. A. *J. Phys. Chem. B* **2003**, *107*, 8158–8165.
- (23) Brûlet, A.; Boué, F.; Cotton, J. P. *J. Phys. II* **1996**, *6*, 885–891.
- (24) Nierlich, M.; Boué, F.; Lapp, A.; Oberthür, R. *Colloid Polym. Sci.* **1985**, *263*, 955.
- (25) Carlsson, F.; Malmsten, M.; Linse, P. *J. Am. Chem. Soc.* **2003**, *125*, 3140–3149.
- (26) Ulrich, S.; Seijo, M.; Laguerre, A.; Stoll, S. *J. Phys. Chem. B* **2006**, *110*, 20954–20964.
- (27) Makowski, H. S.; Lundberg, R. D.; Singhal, G. S. (EXXON Research and Engineering Co.) U.S. Patent 3,870,841, **1975**.
- (28) Essafi, W.; Lafuma, F.; Williams, C. E. *J. Phys. II* **1995**, *5*, 1269.
- (29) Spiteri, M. N.; Williams, C. E.; Boué, F. *Macromolecules* **2007**, *40* (18), 6679–6691.
- (30) (a) Mendes, E.; Girard, J. B.; Picot, C.; Buzier, M.; Boué, F.; Bastide, J. *Macromolecules* **1993**, *26*, 6873–6877. (b) Bastide, J. Candau, S. J. In *Physical Properties of Gels*; Cohen-Addad, J. P., Ed.; John Wiley & Sons: New York, 1996.
- (31) We used long recording times to get very small statistical errors (error bars are smaller than symbols in Figures 3, 5, and 6). Then, we have to determine the error resulting from the zero ϕ_D extrapolation, made by linear fitting of $I(q)/\phi_D$ at each value of q . For that, we try to be as exacting as possible and use the two zero extrapolations corresponding, respectively, to the highest slope and the lowest slope which can be drawn through the data points. We have sometimes rejected some experimental values for the lowest Φ_D (0.25), mostly because a small difference in sample preparation could affect the scattering too much (e.g., for pure polyelectrolyte solutions, see Figure 3). Error bars are larger when the structure factor has a larger effect on the total scattering, i.e., for the globular structure.
- (32) Kratky, O.; Porod, G. *Recl. Trav. Chim. Pays-Bas* **1949**, *68*, 1106–1123.
- (33) Sharp, P.; Bloomfield, V. A. *Biopolymers* **1968**, *6*, 1201–1211.
- (34) des Cloizeaux, J. *Macromolecules* **1973**, *6* (3), 403.
- (35) We get $I(0) = \Phi N_w \Delta \rho^2$ ($P(q) = 1$ at $q = 0$). Taking a density of 1.1 for PSS and the molar mass of d-PSS of 213 g/mol, we get $\Phi = 0.0193$ for a concentration of 0.1 mol/L of PSS repetitions units and $N_w = 2.57 \times 10^{-19} \text{ cm}^{-3}$ for $N = 800$. Since $\Delta \rho^2 = 1.49 \times 10^{21} \text{ cm}^{-4}$, we finally have $I(0) = 7.4 \text{ cm}^{-1}$. This is the value we used to fit data in absolute scale.
- (36) Odijk, T. *Macromolecules* **1979**, *12*, 688–693.
- (37) Dobrynin, V. A.; Rubinstein, M.; Obukhov, S. P. *Macromolecules* **1996**, *29* (8), 2974–2979.

MA702242D